The ISME Journal (2013) 7, 2178–2191

www.nature.com/ismej

OPEN

ORIGINAL ARTICLE

Dynamic cyanobacterial response to hydration and dehydration in a desert biological soil crust

Lara Rajeev[1,6], Ulisses Nunes da Rocha[2,6], Niels Klitgord[3,6], Eric G Luning[1], Julian Fortney[2], Seth D Axen[4], Patrick M Shih[4], Nicholas J Bouskill[2], Benjamin P Bowen[3], Cheryl A Kerfeld[4], Ferran Garcia-Pichel[1,5], Eoin L Brodie[2], Trent R Northen[3] and Aindrila Mukhopadhyay[1]

[1]*Physical Biosciences Division, Lawrence Berkeley National Laboratory, Berkeley, CA, USA;* [2]*Earth Sciences Division, Lawrence Berkeley National Laboratory, Berkeley, CA, USA;* [3]*Life Sciences Division, Lawrence Berkeley National Laboratory, Berkeley, CA, USA;* [4]*Genomics Division, Lawrence Berkeley National Laboratory, Berkeley, CA, USA and* [5]*School of Life Sciences, Arizona State University, Phoenix, AZ, USA*

Biological soil crusts (BSCs) cover extensive portions of the earth's deserts. In order to survive desiccation cycles and utilize short periods of activity during infrequent precipitation, crust microorganisms must rely on the unique capabilities of vegetative cells to enter a dormant state and be poised for rapid resuscitation upon wetting. To elucidate the key events involved in the exit from dormancy, we performed a wetting experiment of a BSC and followed the response of the dominant cyanobacterium, *Microcoleus vaginatus, in situ* using a whole-genome transcriptional time course that included two diel cycles. Immediate, but transient, induction of DNA repair and regulatory genes signaled the hydration event. Recovery of photosynthesis occurred within 1 h, accompanied by upregulation of anabolic pathways. Onset of desiccation was characterized by the induction of genes for oxidative and photo-oxidative stress responses, osmotic stress response and the synthesis of C and N storage polymers. Early expression of genes for the production of exopolysaccharides, additional storage molecules and genes for membrane unsaturation occurred before drying and hints at preparedness for desiccation. We also observed signatures of preparation for future precipitation, notably the expression of genes for anaplerotic reactions in drying crusts, and the stable maintenance of mRNA through dormancy. These data shed light on possible synchronization between this cyanobacterium and its environment, and provides key mechanistic insights into its metabolism *in situ* that may be used to predict its response to climate, and or, land-use driven perturbations.

The ISME Journal (2013) **7,** 2178–2191; doi:10.1038/ismej.2013.83; published online 6 June 2013
Subject Category: Integrated genomics and post-genomics approaches in microbial ecology
Keywords: biological soil crust; desiccation survival; dormancy; *Microcoleus vaginatus*; pulsed-activity event; resuscitation

Introduction

Biological soil crusts (BSCs) are phototroph-driven microbial communities that cover extensive portions of the world's arid and semi-arid deserts and are often dominated by cyanobacteria (Pointing and Belnap, 2012). BSCs can be considered ecosystem pioneers, being the first primary producers, fixing carbon and increasing soil organic matter that reduces wind and water erosion (Belnap and Gillette, 1998; Kidron and Yair, 2001; Belnap *et al.*, 2007). Their colonization of these desert soils may facilitate the subsequent growth of vascular plants by providing and recycling critical nutrients (Mayland and McIntosh, 1966) and have a major role in the nitrogen balance of these ecosystems (Strauss *et al.*, 2011). However, BSCs are sensitive to both physical disturbances and to alterations in temperature or precipitation (Belnap *et al.*, 2004; Kidron *et al.*, 2012; Kuske *et al.*, 2012), and the natural time scale for their recovery range in years to decades (Belnap and Warren, 2002; Kidron *et al.*, 2008). Clearly, a better understanding of the environmental factors that influence the growth and metabolism of BSCs will improve our ability to predict the impacts of global or land-use change on these systems and to develop management strategies to restore BSCs following large-scale disturbances.

Correspondence: TR Northen, Life Sciences Division, Lawrence Berkeley National Laboratory, Berkeley, CA 94720, USA.
E-mail: TRNorthen@lbl.gov
A Mukhopadhyay, Physical Biosciences Division, Lawrence Berkeley National Laboratory, 1 Cyclotron Road, Berkeley, CA 94720, USA.
E-mail: AMukhopadhyay@lbl.gov
[6]These authors contributed equally to this work.
Received 5 March 2013; accepted 21 April 2013; published online 6 June 2013

Microcoleus vaginatus, a filamentous cyanobacterium, is the dominant member of early successional stage BSC communities found in cold deserts of the Colorado plateau (Garcia-Pichel *et al.*, 2001), and one of the most common BSC members worldwide. This organism synthesizes a polysaccharide sheath that bundles many filaments together, efficiently binding particles of sand and soil, stabilizing the substrate and forming the matrix of the early stage BSC (Garcia-Pichel and Wojciechowski, 2009). *M. vaginatus* is able to rapidly resuscitate from and reenter a stress-resistant dormant state during brief periods of hydration (Garcia-Pichel and Belnap, 1996) that favor dormancy strategies over sporulation. *M. vaginatus* is thought to remain in a desiccated and metabolically inactive state below the soil surface during the dry periods that dominate much of the year in these ecosystems (Brock, 1975). During the infrequent rainfall events, *M. vaginatus* exhibits a form of hydrotaxis (Garcia-Pichel and Pringault, 2001; Pringault and Garcia-Pichel, 2004), where they migrate to the surface of the crust causing a visible greening of the surface (Supplementary video 1). Inevitably, desiccation follows and *M. vaginatus* migrates back below the crust surface, entering a dormant state, yet remains poised to resume growth upon wetting.

Desiccation tolerance has been studied in other cyanobacteria (Potts, 1994), including *Nostoc commune* (Billi and Potts, 2002), and the endolithic *Chroococcidiopsis spp*. (Billi, 2009), as well as other bacteria including the radiation-resistant *Deinococcus radiodurans* (Slade and Radman, 2011), actinomycetes (LeBlanc *et al*., 2008) and *Bacillus* spores (Granger *et al*., 2011). In general, these reports suggest that desiccation leads to damage of cell membranes, nucleic acids and proteins, primarily because of oxidative stress (Franca *et al*., 2007) that results from the release of reactive oxygen species (ROS) during desiccation, which is exacerbated under conditions of high light and UV irradiation, typical characteristics of a dehydrating BSC. Known or suspected strategies for desiccation tolerance include mechanisms to prevent or reverse ROS damage, mechanisms for osmoprotection by accumulation of compatible solutes like trehalose and sucrose, and the production of exopolysaccharides that slow the speed of water loss (Billi and Potts, 2002).

That *M. vaginatus* can rapidly migrate to the soil surface following rehydration, and retreat in response to impending desiccation (Garcia-Pichel and Pringault, 2001; Pringault and Garcia-Pichel, 2004), suggests that it possesses a coordinated, and possibly anticipatory, response strategy to these sporadic precipitation events. This anticipatory regulation cannot be based on other known cyanobacterial master regulators, like those involved in internal clocks (Golden and Canales, 2003), because the duration and frequency of the wetting events are unpredictable. The questions remain: how does this cyanobacterium rapidly restart its metabolism after prolonged dormancy, and how does it prepare for inevitable desiccation? Many aspects of these processes remain unknown or poorly characterized, the exit from dormancy having been studied in only a few microbial systems such as in *Actinobacteria* and germinating *Bacillus* and fungal spores (Dworkin and Shah, 2010).

Historically, the search to reveal mechanisms that control important functions in microbe-dominated ecosystems is biased towards studies that focus on the key organism in axenic cultures (reviewed by Hardoim *et al.* (2008)). Laboratory cultivation may result in the evolution of the model organisms towards the well-defined growth conditions typically used (reviewed by Gibbs (1999)), which in turn may influence the microbial response towards the stress being examined. Microorganisms may function differently when studied in axenic cultures versus in their natural environment not only because of ecological interactions with a complex microbial community but also because of the abiotic environment that are challenging to mimic in a laboratory setting. Moreover, research pertaining to desiccation of bacteria is often focused on a single function or a small set of functions and may not consider the genome-wide response of the model organism.

Here we report the genome-wide response of *M. vaginatus* wild populations to a controlled *in situ* hydration–dehydration cycle in their natural habitat and complex microbial community. This experiment was performed in the laboratory simulating the wetting event that might be brought about by the passage of a rain front, but with controlled temperature, light cycle and crust hydration. We used BSC samples collected from a cold desert near Moab, UT for these experiments. In addition to monitoring pH, oxygen in the crust interior as well as net CO_2 fluxes, aliquots of soil were destructively harvested for *M. vaginatus* whole-genome expression analysis over a 6-day period. These data were used to construct a conceptual model of the molecular events that occur during this dynamic period. Multivariate statistical analysis was used to resolve the temporal expression patterns starting from the early events that characterize the reinitiation of metabolism immediately following wetting, to the main metabolic pathways expressed in the hydrated and fully active *M. vaginatus*, and finally the key responses that characterize this organism's preparation for desiccation.

Materials and methods

Sample collection

Petri dishes ($6 \times 1\,cm^2$) were used to core and transport samples of BSCs from the Green Butte Site near Canyonlands National Park (38°42′53.9"N, 109°41′34.6"W, Moab, UT, USA). All samples were

taken from a circular area of 3 m radius and were 1 cm deep. Details on the sampling site, sampling methodology and storage of the samples prior experiment can be found elsewhere (Strauss *et al.*, 2011). Samples were transported air-dry, and maintained in the dark under an atmosphere in equilibrium with LiCl desiccant until experimentation (~1.5 weeks).

Wet-up and dry-down

To recreate field conditions, a microcosm room was assembled, where we reproduced the conditions of a rain event equivalent to a 3-day rainy weather system. Although infrequent and shorter wetting events are most common in the desert, larger storms result in such prolonged periods of wetting (Supplementary Data). The microcosm room lacked windows and sun light was mimicked using 400 W lamps, ~40 cm from the samples achieving ~600 μmole photons $m^{-2}s^{-1}$, typical of an overcast summer day in Moab. Dusk and dawn were simulated using a 400-W lamp situated ~2 m from the samples (~24 μmole photons $m^{-2}s^{-1}$). Day, dusk, night and dawn cycles lasted 11, 2, 9 and 2 h, respectively. Rainfall was simulated by addition of 10 ml of ultra-pure water simultaneously to each crust sample and moisture lost due to evaporation was replenished as needed every 6 h to a total of 3.5 mm. During the wet-up, crust material from three biological replicates (three individual pre-sampled petri dishes chosen at random) was collected at: 0 h (before wetting sample), 3 min (immediately after wetting), 15 min, 1 h, 9 h (day), 11.5 h (dusk), 18 h (night), 22 h (dawn), 25.5 h, 31.5 h (day), 35.5 h (dusk), 42 h (night) and 49.5 h (day). Drying was then initiated at 72 h by the removal of surface water, and was assisted by decreasing the humidity of the room through the use of air conditioners. Crust material from three biological replicates was collected at 1 and 2 h following removal of water when the crust was still moist, at 4 h when the crust appeared semi-dry, at 8 h when the crust was visibly dry, and a final fully dry sample 3 days later. All samples were immediately frozen in liquid nitrogen and stored at −80 °C until RNA extraction.

Biogeochemical measurements

Simultaneous pH and O_2 analysis was performed on a separate BSC sample using microelectrodes. Oxygen concentration was monitored continuously at the surface of the crusts using a fiber optic-based microoptode sensor system (Microx, Precision Sensing GmbH, Regensburg, Germany), placed using a motorized micromanipulator, and operated according to manufacturer's specifications. Sensor's fibers had their tips coated with a fluorescent dye that can be quenched by oxygen (Klimant *et al.*, 1995). The signal was 2 point calibrated against air-bubbled, fully oxygenated water (100% saturation) and N_2-flushed water (0% saturation). Data were digitized and reported at 5 min intervals. Following calibration in two buffers (pH 4.0 and 10.0), pH measurements were made at 3 s intervals using PH-50 microelectrodes (Unisense, Aarhus, Denmark). Current was measured with a Unisense microsensor multimeter and recorded using SensorTracePRO software (Unisense). As we used microelectrodes to constantly measure O_2 and pH, these measurements were interrupted once the dry-down started. Temperature was measured with five sensors placed randomly at the same distance from the light source as the BSC samples.

A separate set of samples was used to determine CO_2 flux. Four biological replicates were sealed with 100 ml mason jars connected to a Micro-Oxymax Respirometer (Columbus Instruments, Columbus, OH, USA) with a time resolution of 42 min per replicate. These values were scaled to units of $g\ m^{-2}h^{-1}$ and the values in Figure 1 are the means of the four replicates (Supplementary Table S1). The maximum values of CO_2 production were between 0.03–0.05 g CO_2 $m^{-2}h^{-1}$, and minimal values (that is, uptake) between −0.06 and −0.10 g CO_2 $m^{-2}h^{-1}$ (Supplementary Table S1). After initiating the dry-down the samples used to measure CO_2 flux were removed from the jars to allow the water to evaporate. Therefore, CO_2 flux measurements during the dry-down were more intermittent than during the wet part of the experiment.

The crust water activity was measured using an Aqualab Dew Point Water Activity Meter (Decagon Devices Inc, Pullman, WA, USA) and converted to water potential according to the manufacturer's instructions (Supplementary Table S2 and Supplementary Figure S1).

RNA extraction and microarray analysis

Total DNA and RNA were co-extracted from BSC samples using a modified CTAB/phenol–chloroform method as described (Placella *et al.*, 2012) (SI Methods). The extracted RNA was DNAse treated using Turbo DNA-free DNAse (Life Technologies, Grand Island, NY, USA), and the DNA-free RNA (50 ng) was amplified using the Sigma Whole-Transcriptome Amplification 2 kit (Sigma-Aldrich, St Louis, MO, USA). The resulting cDNA was cleaned up using Qiaquick PCR clean up kit (Qiagen Inc, Valencia, CA, USA), and was labeled with Cy3 9-mers using One color DNA labeling kit (Roche-Nimblegen, Madison, WI, USA) following the manufacturer's protocol. Four microgram of the labeled cDNA was hybridized at 42 °C overnight to a custom Roche-Nimblegen microarray. *M. vaginatus* is the dominant taxon in this metagenome (Supplementary Figure S2) and the array was designed using 42499 60-mer oligonucleotide probes in triplicate that represent 6130 *M. vaginatus* genes (7 probes per gene), with 5461 sequences from strain PCC 9802 and 669 sequences from strain FGP-2

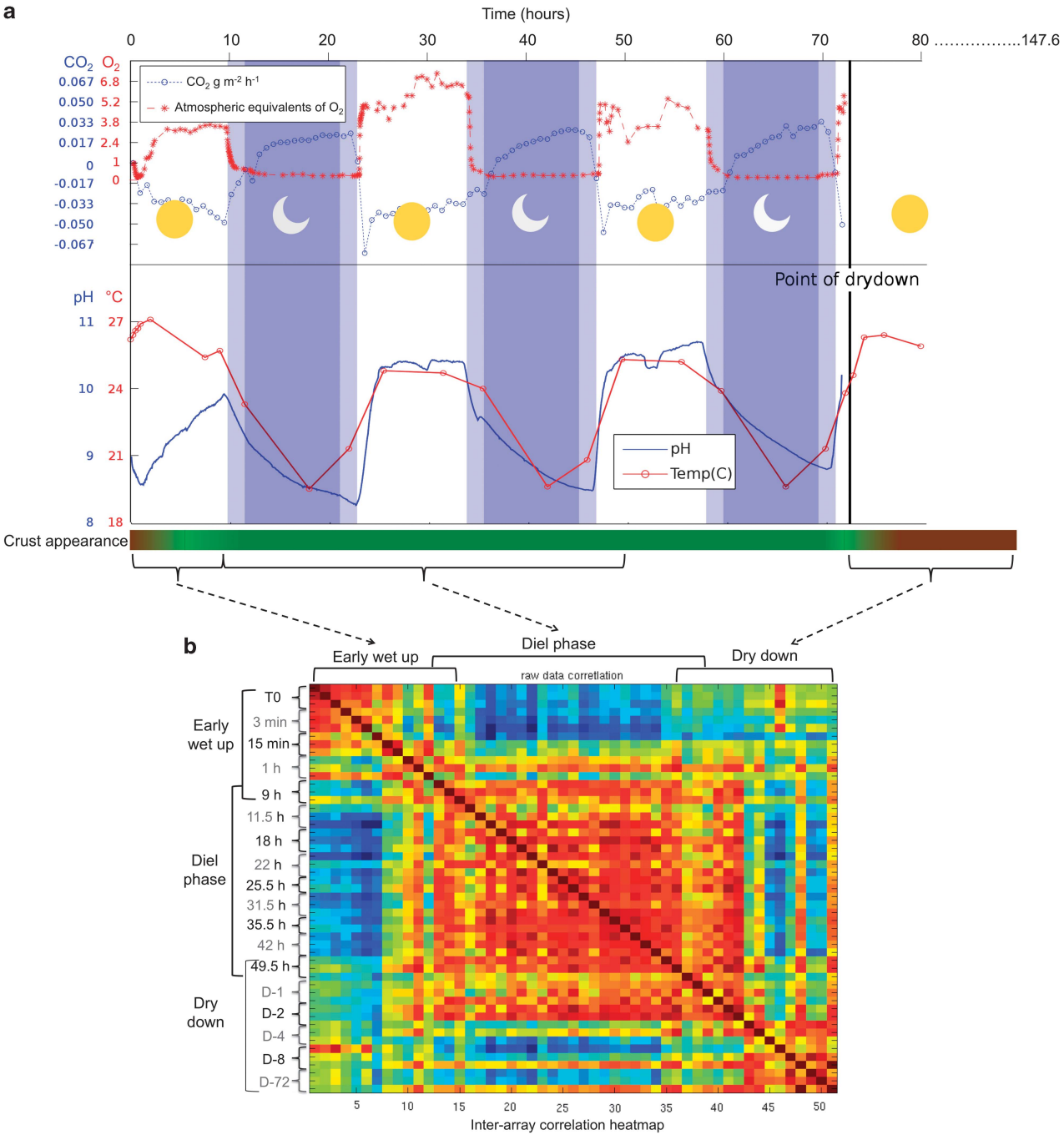

Figure 1 Simulated hydration–dehydration cycle in a BSC sample. (**a**) Measurements of CO_2 flux, O_2 partial pressures, pH and temperature of BSC samples over a hydration period of 72 h with day–night cycles. Dusk and dawn simulations are indicated by the light purple shading and night by the dark purple shading. The schematic of the BSC appearance indicates greening of the crust within a few minutes of wetting, which reversed within a few hours of the start of the drying. (**b**) Inter-array correlation map of all replicates in all time-points (three replicates per time point, except for 25.5 h, 35.5 h and D-4 h that have two replicates each), showing three blocks of correlation forming the early-wet-up, the diel phase and the dry-down blocks. The heatmap also demonstrates heterogeneity within individual replicates of a single-time point, where some correlate better with earlier or later time points than to their contemporaries.

(Starkenburg *et al.*, 2011). The slides were scanned at 532 nm using the GenePix 4200A scanner (Molecular Devices, Sunnyvale, CA, USA). The images were gridded and pair files generated using the Nimblescan software version 2.4 (Roche-Nimblegen). All replicates for all time points (only two replicates were used for the 25.5 h wet-up, and 4 h dry-down time points owing to poor array quality of the third replicate) were normalized together by RMA (robust multi-chip average) analysis using Nimblescan. The array data have been deposited in NCBI's Gene Expression Omnibus (accession number: GSE40188).

Microarray correlation analysis
Each pair of normalized microarray expression values were then compared using correlation with a Euclidean distance in Matlab (Mathworks, Natick, MA, USA). Correlation distances were then visualized in an array-by-array matrix. Arrays that correlated weakly with their replicates (one replicate at 35.5 h) were removed from further analysis. As three blocks of correlation separating the early time points, the intermediate diel cycle time points and the dry-down time points were clearly identifiable, we partitioned the data and analyzed these three groups in parallel.

Selection of genes for profile clustering
In each of the three blocks of correlation, we identified the genes that were most robustly varying within the arrays. We used the RMA-normalized expression values to calculate the pooled s.d. for each gene on the microarray using the pooled variance method. The mean expression of each gene at each sample point was calculated. The mean time-point expression was used to calculate the profile deviation (s.d. of expression across time-points). The genes with a profile deviation greater than 1.25-fold their pooled s.d. were selected for profile building. This resulted in a core set of genes: 883 for the early wet-up block, 80 for the diel phase block, and 201 for the dry-down phase (Supplementary Tables S3, S4, S5).

Gene profile clustering
Expression profiles of each gene were further normalized to be centered (zero mean) and unit length. *k*-Means clustering was then applied to gene expression profiles previously selected using correlation distance, and used 1000 replicates to build $k = 1$–12 clusters. Mean cluster patterns were then inspected, selecting $k = 5$, 3, 5 as the most informative partitioning for the early, diel and late regimes, respectively. The mean cluster profile was then generated by finding the mean expression value at each time-point for the genes within a cluster.

Gene profile cluster mapping
To understand how genes were behaving within each temporal-regime, we mapped each gene back to a profile cluster. To account for genes that might not map well to any cluster (that is, be negatively correlated with all clusters) we introduced a null-cluster profile representing no expression change. The correlation distance of each gene expression profile to each mean cluster profile was calculated, and each gene was assigned to its closest cluster profile (Supplementary Table S6).

Cluster functional enrichment
Gene sequences corresponding to the probes on the microarray were mapped to KEGG Orthology IDs using the KEGG Automatic Annotation Server (KAAS), which allows for the mapping of a gene to one or more KEGG pathway. Each cluster was then checked for enrichment of KEGG pathways using the hypergeometric distribution.

Results

Biogeochemical observations during the wet-up and dry-down experiment
Samples of early successional stage BSC were harvested from an existing field site near Moab, UT, USA. After addition of water to the crust samples, the surfaces became noticeably green within 15 min, and small bubbles, presumably O_2, were observed effervescing at the surface of the BSC within 45 min (Supplementary video 1). There was visible heterogeneity in the extent of greening observed across the different samples.

Soil solution oxygen concentration measurements indicated severe oxygen depletion in the crusts within the first few minutes after wetting, followed by a steady increase up to 3.7 atmospheric equivalents of O_2 (Figure 1a). Subsequently, oxygen concentrations followed a diurnal pattern. Sharp declines in production were observed at the day-to-dusk transition, with the soil solution becoming anoxic at night, followed by sharp increases at the dawn-to-day transition. Higher steady-state oxygen concentrations (up to 6.9 atmospheric equivalents, or 1.4 atm) were observed during the second day compared with the first (Figure 1a).

Carbon dioxide measurements indicated that CO_2 uptake began during the first hour. On the first day, CO_2 fixation increased until dusk, when it declined sharply and net efflux (respiration) was observed during the nighttime coinciding with oxygen depletion (Figure 1a). Net CO_2 uptake was observed again at the start of day 2, coincident with the onset of photosynthetic oxygen evolution (Figure 1a). Diel cycles of temperature ranged from 19 to 27 °C (Figure 1a). The pH measurements also showed a diurnal pattern, with a pH of up to 10.7 during photic periods, and decreasing to 8.4 in the dark phases (Figure 1a). All of these changes in microenvironmental conditions are consistent with earlier reports in similar crusts (Garcia-Pi**c**hel and Belnap, 1996).

Following the removal of surface water, crusts became visibly dry over a 6 h period and developed a more gelatinous appearance (Supplementary video 2). The filamentous cyanobacteria retreated below the surface, visible as a reversal of the initial 'greening'. The early stage of dry-down showed a characteristic decline in bulk sample water potential over 3 h from ~ 0.30 to -5.0 MPa (Supplementary Table S2 and Supplementary Figure S1). After 24 h of drying, water potentials approached -80 MPa (Supplementary Table S2). Subsequent time points showed a cyclical pattern with water potentials

increasing in the early morning measurements, possibly as a result of equilibration with room humidity in the transition from day to night (Supplementary Figure S1). Periodic CO_2 flux measurements during the drying indicated continued CO_2 fixation during daytime, with respiration in the morning time points (Supplementary Table S1).

Temporal gene expression analysis

Inter-array correlation analysis with an array-by-array matrix revealed three correlation groups that separated the transcriptional responses of the early wet-up, the intermediate diel cycle and late dry-down time points (Figure 1b). K-means cluster analysis on the three phases in parallel (see methods, Figures 2a–c) defined five clusters, A1–A5, in the early wet-up group (Figure 2a), three clusters, B1–B3, for the diel phase group (Figure 2b), and another five clusters, C1–C5, for the dry-down group (Figure 2c).

A comparison of the clusters in the early wet-up and dry-down groups revealed clear patterns. There was significant enrichment of genes found in the early clusters A4 and A5 that increased in expression upon hydration and the dry clusters C4 and C5 that decreased in expression during dehydration (Tables 1 and Supplementary Table S7). These clusters included the majority of genes with KEGG assignments in the major metabolic pathways (Table 1). The early clusters A1 and A2 that decreased in abundance upon wetting had strong overlaps with dry clusters C1, C2 and C3 whose expression increased during drying (Supplementary Table S7).

Early events in M. vaginatus upon crust hydration

Starting from T0, the first 9 h post wet-up marked the early events of crust hydration (Figure 2a). Genes in cluster A1 decreased in expression immediately upon wetting, and overlap with those that increased in expression during drying, and are therefore discussed in detail in the later section; transcriptional events during drying. Genes in clusters A2 and A3 showed transient increases in expression at 3 and 15 min post wetting respectively. Cluster A2 included genes encoding signaling/regulatory proteins, and a few genes possibly involved in DNA repair (Figure 3a, Supplementary Table S8). Cluster A3 included DNA repair genes (*mutT, recJ* and *recR*), genes with DNA-binding domains and pentapeptide repeat genes that may be DNA mimics (Hegde *et al.*, 2011) (Figure 3b, Supplementary Table S8). There were also signaling/regulatory genes encoding alternate RNA polymerase sigma factors, or involved in cyclic nucleotide signaling or two component systems with possible functions in light sensing, chlorophyll metabolism or chemotaxis (Supplementary Table S8).

As early as between 3 and 15 min of wetting, genes in most major metabolic pathways were induced (Clusters A4 and A5, Table 1). These included genes in photosynthesis (allophycocyanin antenna genes, and a few PSII and electron transfer genes), chlorophyll synthesis, glycolytic and pentose phosphate pathways, respiration, nitrogen assimilation, fatty acid metabolism, synthesis of exopolysaccharides and storage molecules (Supplementary Table S9). Genes for the transport of various nutrients such as phosphate, bicarbonate, sulfate, nitrogen sources (nitrate, ammonium, urea), sugars, amino acids, spermidine, ferric and cobalt ions were also induced (Supplementary Table S9).

Diel-regulated transcriptional events

The fully hydrated crust displayed characteristic diel behavior (Figures 2b and 4, Supplementary Table S10). The bicarbonate transport genes and the carbonic anhydrase gene cluster were maximally expressed during the day, whereas the carboxysome structural genes (*ccm* operon) were induced at night (Figure 4). In the Calvin cycle, RubisCo and phosphoribulokinase genes showed a slight increased expression during the photic periods. Only two photosystem genes (encoding a PSII protein and the PsaL protein) expressed in a putative operon showed a diel pattern. The light-dependent protochlorophyllide reductase gene in chlorophyll synthesis increased in expression during the day, whereas the light-independent enzyme increased in expression at dusk (Figure 4).

The chlorophyll a-/b-binding proteins and orange carotenoid protein encoding genes, the *groES/EL* chaperones and some oxidative stress protection genes, including a superoxide dismutase, followed a day cycle (Figure 4, Supplementary Table S10). Additionally, an FeS cluster assembly operon *sufSDCB* was highly induced during the day, and an associated *sufR* regulatory gene showed a similar pattern (Figure 4).

Some genes in the pentose phosphate pathway, glycogen breakdown and respiration followed a dusk or night cycle (Figure 4). An interesting cluster of predicted gas vesicle proteins were induced at dusk or night times (Figure 4). Several regulatory genes also followed a diel cycle (Supplementary Table S10).

Transcriptional events during drying

Most molecular events that mark the reentry into desiccated state (Figure 2c) were completed within 8 h of water removal. Expression of genes in the majority of central anabolic pathways were repressed within 1–2 h following the removal of surface water from the crust (See Table 1 for enrichment of KEGG metabolic pathways in clusters C4 and C5).

Genes for the synthesis of compatible solutes such as trehalose and sucrose, as well as sugar transporters and K^+/H^+ or Na^+/H^+ antiporters

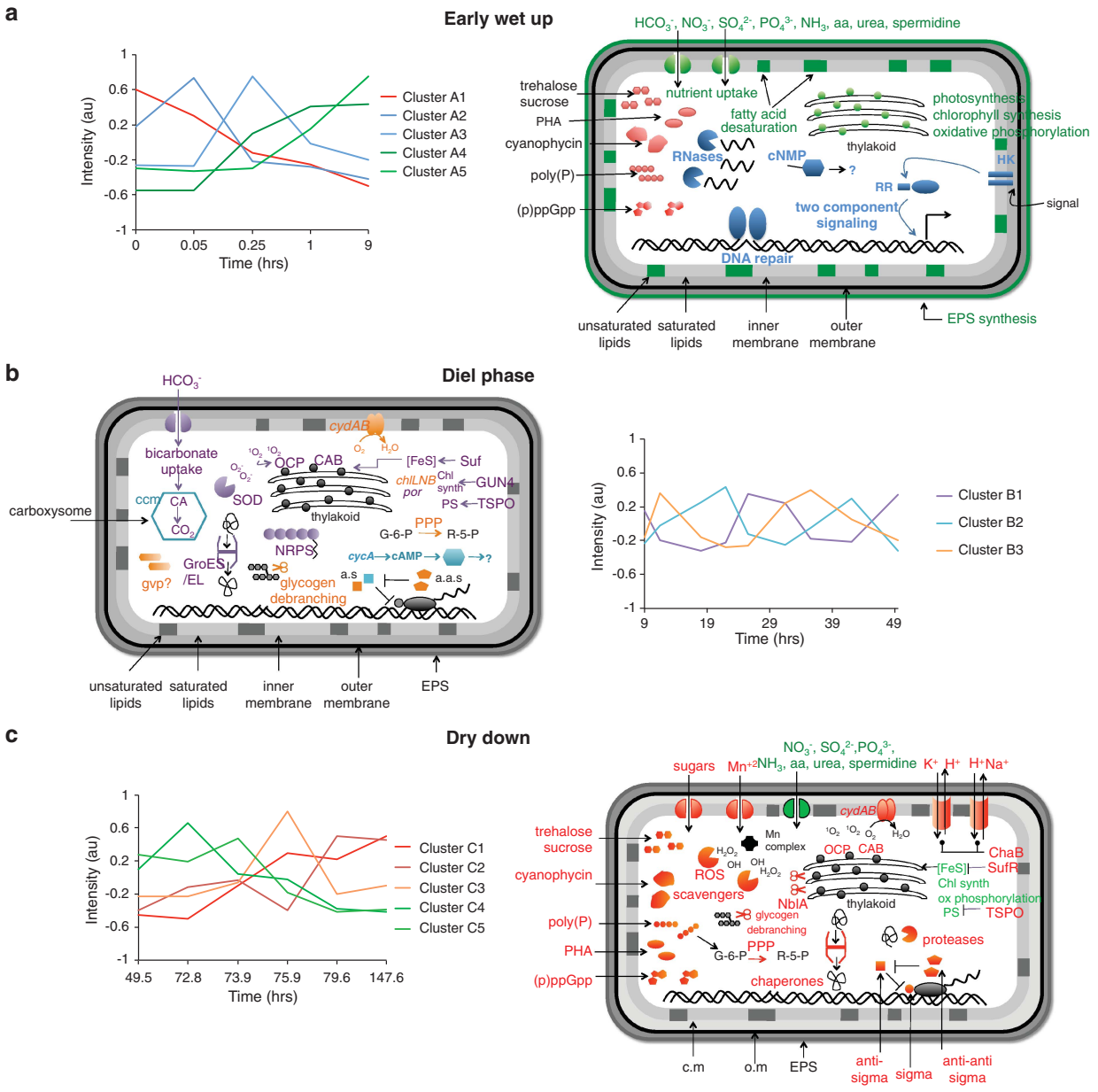

Figure 2 Transcriptional response of *M. vaginatus* in the BSC to the simulated hydration–dehydration event. Graphs represent *k*-means clustering of expression profiles and the cell diagrams depict the conceptual models showing the key transcriptional events in the early wet-up block 0–9 h (**a**), in the diel phase block from 9–49.5 h (**b**) and in the dry-down block (**c**). *Y* axis represents the expression intensities in arbitrary units after RMA normalization and centering to zero mean. The similar colors for cluster lines in (**a**, **c**) indicate a high overlap in the genes represented by those clusters between the early wet-up and dry-down blocks. Colors for the cluster lines also match those used in the cell diagrams to represent the same set of genes. In the early wet-up (**a**), DNA repair, signaling via two component systems and cyclic nucleotides, and RNases that are transiently induced in response to wetting are representative of genes in clusters A2 and A3 (blue). Synthesis of compatible solutes and storage molecules are representative of cluster A1 (red) that have decreased abundance on wetting. Nutrient uptake, photosynthesis, chlorophyll metabolism, oxidative phosphorylation, EPS synthesis and fatty acid desaturases are among the genes that are induced in response to hydration in clusters A4 and A5 (green). In the diel phase (**b**), CO_2 uptake and concentration, ROS scavengers (superoxide dismutase SOD, orange carotenoid protein OCP), GroES/EL chaperones, FeS cluster assembly (*suf* genes), nonribosomal peptide synthase (*NRPS*) genes and regulators of chlorophyll synthesis (GUN4) and photosynthesis (TSPO) represent cluster B1 with a day cycle (purple). Structural components of the carboxysome (ccm) and cyclic nucleotide signaling genes (*cycA*) represent cluster B2 with a night cycle (blue), and gas vesicle like genes, cytochrome bd oxidase, pentose phosphate pathway genes, glycogen breakdown and sigma factor regulation represent cluster B3 with a dusk cycle (orange). In the dry-down (**c**), clusters C4 and C5 (green) that decrease in expression upon drying include nutrient uptake, photosynthesis, oxidative phosphorylation and FeS cluster assembly. Clusters C1, C2 and C3 (red) that are induced upon drying include synthesis of trehalose, sucrose, cyanophycin, polyhydroxyalkanoate (PHA), (p)ppGpp, genes utilizing polyphosphate, ROS scavengers, sugar and Mn^{+2} uptake, K^+ and Na^+ antiporters, phycobilisome degradation protein NblA, chaperones, glycogen breakdown, pentose phosphate pathway, proteases and sigma factor regulation.

Table 1 KEGG functional assignments for the different clusters in the early (A1–A6), diel (B1–B4) and dry-down phases (C1–C6)

Pathway	*No. of genes*	*Number of genes in*															
		Early phase clusters						*Diel phase clusters*				*Dry-down clusters*					
		A1	*A2*	*A3*	*A4*	*A5*	*A6*	*B1*	*B2*	*B3*	*B4*	*C1*	*C2*	*C3*	*C4*	*C5*	*C6*
Glycolysis/Gluconeogenesis	25	6	0	2	2	15	0	5	12	8	0	6	0	0	2	17	0
Citrate cycle (TCA cycle)	13	0	1	0	3	9	0	1	7	5	0	1	1	1	2	8	0
Pentose phosphate pathway	21	3	4	3	3	8	0	3	10	8	0	5	3	1	4	8	0
Fatty acid biosynthesis	10	2	3	0	2	3	0	3	6	1	0	0	1	1	4	4	0
Oxidative phosphorylation	33	0	0	2	4	27	0	17	6	10	0	7	0	3	0	23	0
Photosynthesis	42	2	1	2	8	29	0	22	18	2	0	4	4	1	4	29	0
Photosynthesis antenna proteins	13	3	1	2	1	6	0	9	4	0	0	0	2	1	0	10	0
Purine metabolism	43	7	6	9	4	17	0	8	21	14	0	3	3	2	10	25	0
Pyrimidine metabolism	32	5	5	9	2	11	0	4	16	12	0	3	3	1	8	17	0
Peptidoglycan biosynthesis	14	1	2	0	1	10	0	6	5	3	0	0	0	0	7	7	0
Glycerolipid metabolism	10	0	0	0	4	6	0	4	5	1	0	0	0	0	2	8	0
Glycerophospholipid metabolism	8	0	1	1	4	2	0	3	5	0	0	0	1	0	0	7	0
Carbon fixation in photosynthetic organisms	17	5	0	0	4	8	0	3	12	2	0	3	0	0	3	11	0
Carbon fixation pathways in prokaryotes	19	2	3	0	4	10	0	4	10	5	0	4	1	1	6	7	0
Porphyrin and chlorophyll metabolism	46	8	4	9	6	19	0	10	19	17	0	7	6	3	13	17	0
Terpenoid backbone biosynthesis	13	3	2	2	3	3	0	1	10	2	0	1	2	0	1	9	0
Carotenoid biosynthesis	10	1	3	2	3	1	0	6	4	0	0	2	0	1	2	5	0
Nitrogen metabolism	21	4	1	1	8	7	0	9	6	5	1	7	1	1	3	9	0
AminoacyltRNA biosynthesis	25	1	1	4	8	11	0	10	9	6	0	2	1	1	8	13	0
ABC transporters	61	8	8	8	20	17	0	22	24	13	2	2	8	4	15	32	0
Two component system	46	12	9	9	7	9	0	13	20	13	0	6	9	9	12	10	0
Bacterial chemotaxis	6	3	2	1	0	0	0	3	1	2	0	0	1	5	0	0	0
Ribosome	51	12	2	0	1	36	0	5	8	38	0	0	1	4	41	5	0

Abbreviation: TCA, tricarboxylic acid cycle.

increased in expression (Figure 5, Supplementary Table S11). Among reserve polymers, gene clusters for metabolism of cyanophycin and synthesis of polyhydroxyalkanoates were upregulated, (Figure 5) but the breakdown of glycogen was also enhanced. In addition, genes involved in the pentose phosphate pathway and the respiratory cytochrome oxidase genes *coxABC* and *cydA* were also overexpressed (Figure 5). A gene predicted to encode polyphosphate glucokinase, which catalyzes poly(P)-driven formation of glucose-6-P from glucose, was strongly upregulated. Furthermore, a putative operon involved in pentose-glucuronate conversions and some genes predicted to be involved in amino sugar or nucleotide sugar metabolisms were also induced during dehydration (Figure 5, Supplementary Table S11).

Chaperone genes, such as *groES/EL* and *dnaJ-dnaK*, and a putative stress-induced LEA-like (late embryogenesis abundant) protein that has been implicated in reducing desiccation-induced aggregation of cell proteins (Chakrabortee *et al.*, 2012) were induced. Several oxidative stress protection genes were expressed (Figure 5, Supplementary Table S11), such as multiple Mn-containing catalases to scavenge ROS, *dps* (DNA-binding ferritin) genes that protect DNA from oxidative damage (Martinez and Kolter, 1997), and thioredoxin/glutaredoxins and methionine sulfoxide reductases to reverse protein oxidation (Boschi-Muller *et al.*, 2008; Kohárýová and Kolárová, 2008). Genes for photo-protective orange carotenoid proteins and chlorophyll A–B-binding proteins (Kirilovsky 2010) were strongly upregulated. ABC transporter genes for Mn^{+2} ions were among the few transporters that were upregulated during drying (Figure 5) and might be involved in protecting the proteome against oxidative stress by forming Mn-complexes that scavenge ROS as demonstrated for *Bacillus subtilis* (Granger *et al.*, 2011) and *Deinococcus* (Frederickson *et al.*, 2008). The *nblA* gene encoding a phycobilisome degradation protein (Richaud *et al.*, 2001) was highly overexpressed. The putative operon (PSII–*psaL*) and an orphan carbonic anhydrase gene showed low increases in expression.

Among other top differentially expressed genes, there were several genes coding for enzymatic functions such as dehydrogenases, esterases and hydrolases and multiple protease genes. A phospholipid-binding domain protein along with some glycoside hydrolase genes encoded in the same gene cluster were upregulated, as well as a GTP-binding protein and the translation elongation factor *EF-G* genes (Figure 5, Supplementary Table S11).

There were many signaling and regulatory events that appeared to be desiccation specific (Figure 5, Supplementary Table S11): the stringent response alarmone (p)ppGpp synthetase (RelA/SpoT), ChaB cation transport regulators and the iron sulfur cluster biosynthesis regulator *sufR*, in particular.

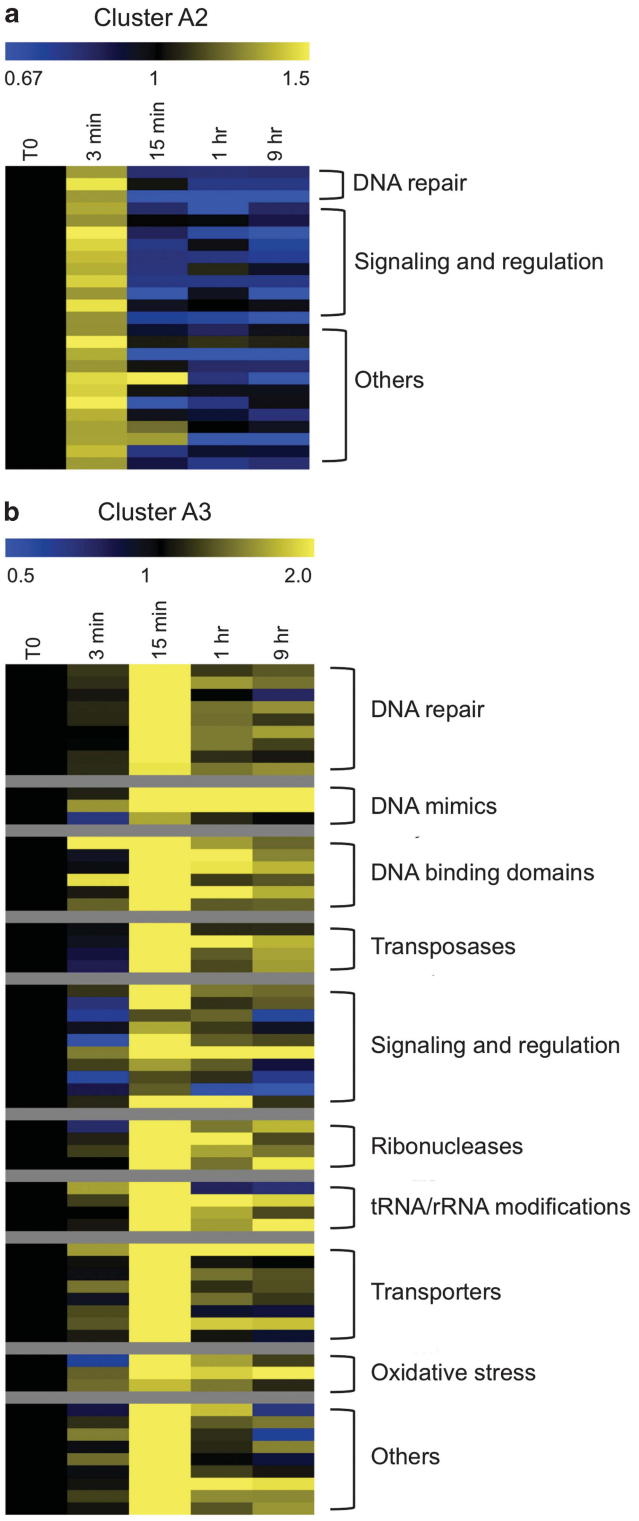

Figure 3 Genes transiently induced during early wet-up time points. (**a**) Genes belonging to cluster A2 showed a low increase in expression immediately upon wetting and include DNA repair and signaling genes. For more detail see Supplementary Table S8. (**b**) Genes belonging to cluster A3 showed a peak in expression at 15 min past wetting and include DNA repair, DNA-binding proteins, possible DNA mimics, signaling events, RNAases, rRNA/tRNA modifications and oxidative stress genes. For details see Supplementary Table S8. Heatmaps depict fold change in normalized expression relative to T0, according to the scale above each.

Discussion

Microorganisms that inhabit arid environments withstand extreme fluctuations in water potential and severe exposure to solar radiation. Microorganisms that routinely survive such conditions may be expected to have developed coordinated dormancy strategies that ensure cellular integrity and the ability to respond rapidly to, or even anticipate, rehydration, which occurs through infrequent rainfall events. Here we report a temporal system-level analysis into how *M. vaginatus*, a major contributor for carbon fixation in light BSC, responds to wetting and desiccation in the context of its natural microbial community.

Our approach of interrogating natural populations of *M. vaginatus* using intact soil crusts has the advantage that they are already adapted to the constraints of their natural habitat. Thus, the use of the intact BSC microbial community allowed us to expose our system to diel patterns comparable to an overcast desert day, while axenic *M. vaginatus* cultures can only withstand light intensity ten times lower than that used in our experiment. We also used a 3-day long rain episode. Such conditions are relatively rare in the desert but do occur (Supplementary Data) and enabled the differentiation of wet-up and dry down vs diel cycle responses. Using these simulated weather conditions, and sampling in a temporal manner over the 6-day experimental period, allowed us to track key transcriptional responses as and when they occurred.

In our simulated rainfall experiment, we observed a rapid recovery of photosynthetic oxygen evolution and CO_2 uptake, and a diel pattern was apparent immediately following a transition from light to dark. The speedy recovery of metabolism was consistent with previous studies on natural crusts (Garcia-Pichel and Belnap, 1996; Harel *et al.*, 2004; Ohad *et al.*, 2010), and was faster than observed in pure culture studies of other organisms (Scherer *et al.*, 1984). Concurrent with our biogeochemical measurements, transcription displayed cyclical patterns of gene expression with exit from dormancy upon hydration, a re-initiation of metabolism and preparation for desiccation. We observed mirrored trends through early stages of wetting and late stages of drying, with strong overlaps among the genes downregulated during drying and those induced during early wetting, and among genes upregulated during drying and those that decreased during early wetting.

Our results suggest the following conceptual model for *M. vaginatus*'s response to hydration and desiccation (Figure 2). Early gene expression events following hydration included (1) a turnover or active downregulation of transcripts that were synthesized during desiccation; (2) increase in expression of genes involved in nutrient uptake, synthesis of chlorophyll and ATP synthesis among others that

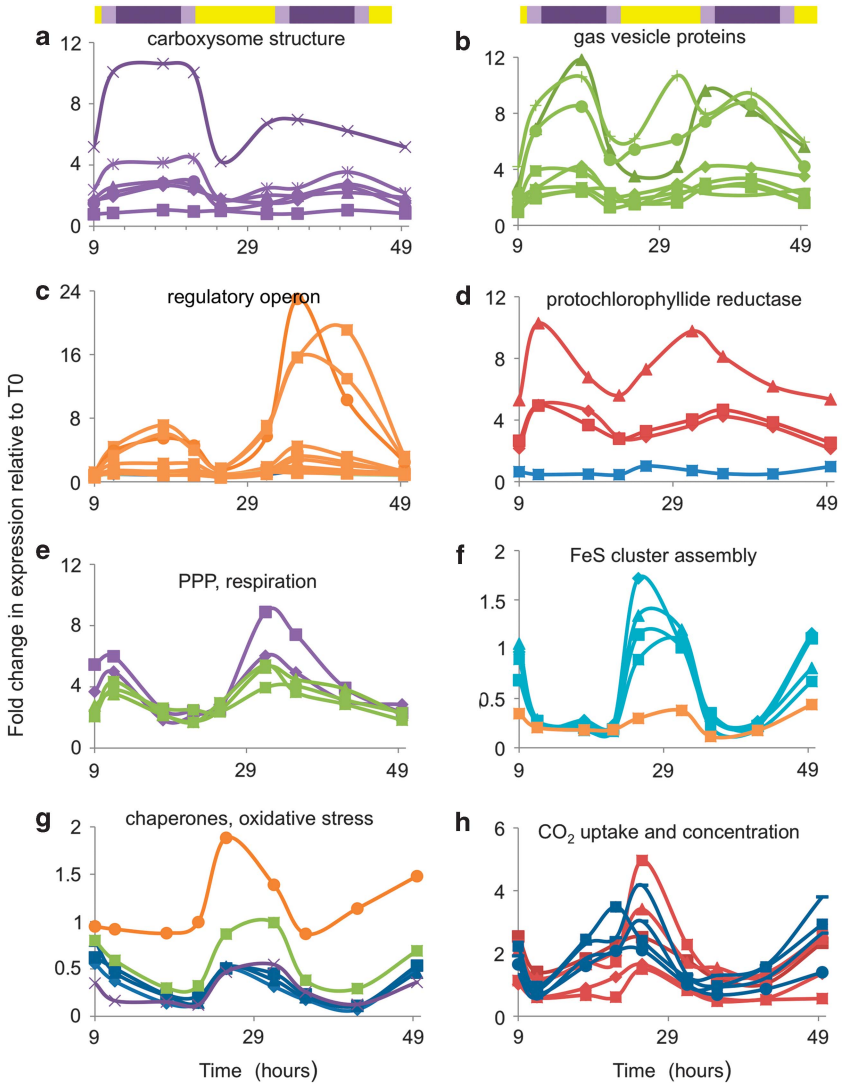

Figure 4 Primary genes displaying differential expression over day–night cycles. (**a**) Structural components of the carboxysome (genes 2505167029-34, purple) showed a preferential nighttime expression. (**b**) Genes encoding gas vesicle-like proteins (2505166061-68, green) had maximal expression at dusk. (**c**) Expression of operon 2505169735-45 (orange), with several sigma factor regulatory genes, also peaked at dusk. (**d**) The three subunits of the light-independent protochlorophyllide reductase (*chlB, chlN, chlL*) (red) had maximum expression at dusk, whereas that of the light-dependent enzyme (blue) peaked during daytimes. (**e**) Pentose phosphate pathway genes (*phosphoketolase, glucose-6-phosphate-1-dehydrogenase* and *6-phosphogluconate dehydrogenase*) (green) as well as the cytochrome d oxidase (*cydAB*) (purple) reached maximal expression at dusk. (**f**) The *sufSDCB* (turquoise) and the *sufR* (orange) genes for FeS cluster assembly had maximum expression during the daytime. (**g**) The *groES/EL/EL2* chaperone genes (blue), and oxidative stress protectants superoxide dismutase (orange), peroxiredoxin (green), glutaredoxin (purple) genes were induced during the day. (**h**) The bicarbonate ABC transporter genes (2505169176-79) (blue) and the carbonic anhydrase gene cluster (2505169834-38) (red) were also maximally induced during the day. For more gene information and a complete list of all genes showing detectable diel gene expression patterns, see Supplementary Table S10. The colored bar on top indicates day–night cycles with yellow blocks indicating daytime and purple blocks indicating dark (short light purple blocks depict dusk and dawn while the longer dark purple blocks depict night).

contribute to the rapid re-initiation of metabolism; and (3) transient increases in expression of genes required to repair the DNA damage caused by desiccation, signaling/regulatory genes that possibly transduce the signals such as water potential change, RNAses for turnover of unnecessary transcripts and rRNA/tRNA modification genes that may be necessary for preparation of translation (Figure 2a).

Following hydration, the cells rapidly (1–9 h) entered a phase of fully active metabolism. Several responses that mapped to this phase may also serve as preparation for a subsequent dehydration event. For example, one of two gene clusters for the synthesis/hydrolysis of cyanophycin (a typical nitrogen reserve; Kolodny *et al.*, 2006) was expressed only upon hydration. Polyphosphate, also a storage molecule, may be continuously synthesized using the two polyphosphate kinase genes *ppk1* and *ppk2*, as they are expressed but did not appear to be differentially regulated. Concentrations of polyphosphate may be controlled by the

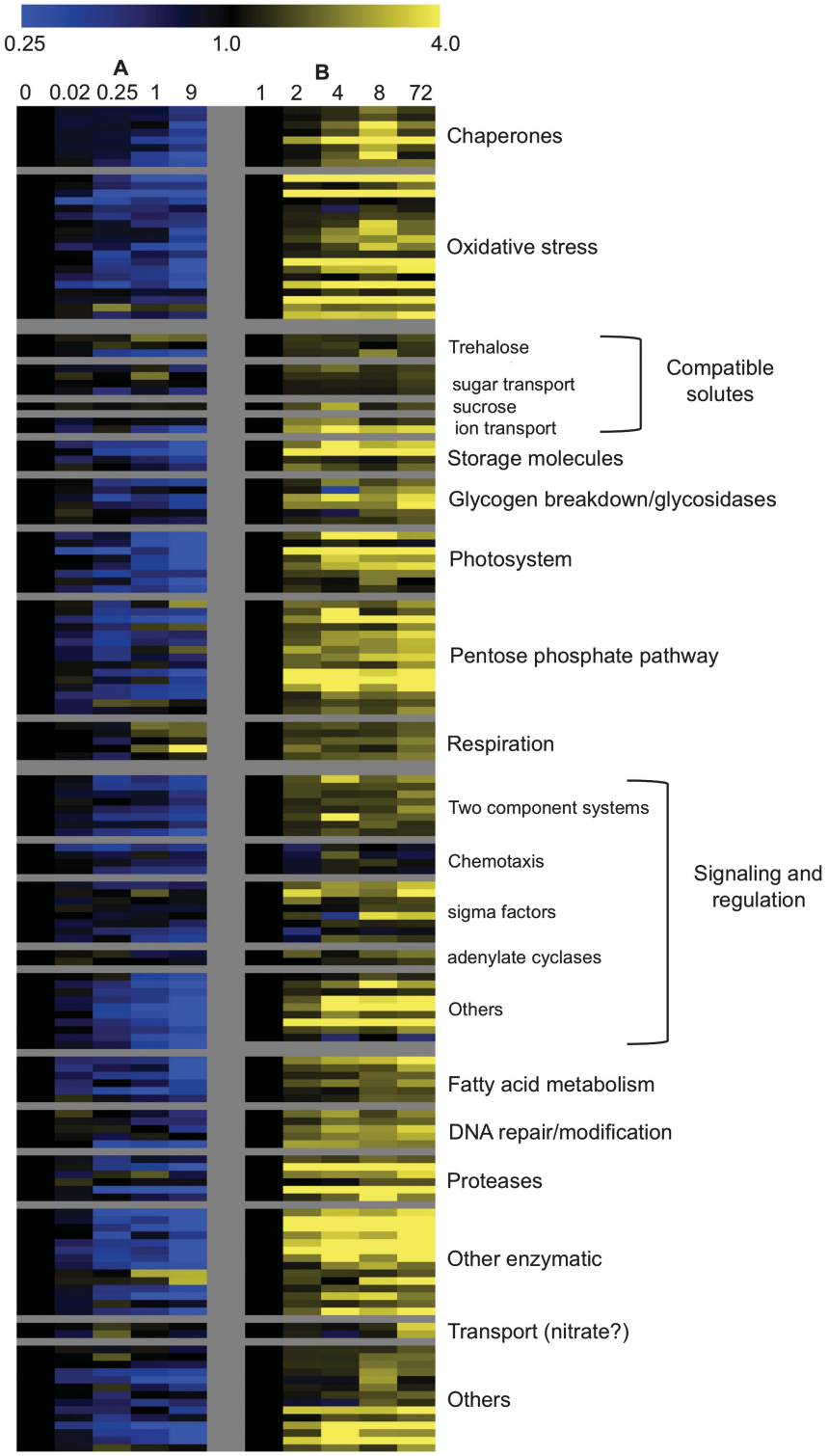

Figure 5 Transcripts that downregulate upon wetting (**a**) are induced again at onset of desiccation (**b**). These include chaperones, oxidative stress protectants, synthesis and transport of compatible solutes, synthesis of storage molecules, glycosidases, proteases and other enzymes, photosystem genes, pentose phosphate pathway and pentose-glucuronate conversion genes, respiration, fatty acid metabolism, some DNA modifications, and several signaling and regulatory genes. The heatmap denotes fold change in normalized expression relative to T0 for the early wet-up time points T0,.02,.25, 1 and 9 h (**a**), and fold change in expression relative to the first dry-down time point for the times 1, 2, 4, 8 and 72 h past start of dry-down (**b**). For gene details see Supplementary Table S11.

exopolyphosphate *ppx* gene levels, which increased upon wetting, and through (p)ppGpp (Kuroda *et al.*, 1997) the synthesis of which was induced during desiccation. Induction of genes for exopolysaccharide synthesis upon hydration (Figure 2a) may be important in contributing to desiccation tolerance

by protecting cell membranes (Hill *et al.*, 1997; Tamaru *et al.*, 2005). Also, exopolysaccharide synthesis may facilitate the motility of *M. vaginatus* as previously observed (Campbell, 1979). Genes for fatty acid desaturation, which were highly over-expressed upon wetting (Figure 2a), may aid in desiccation resistance as a result of altered, possibly increased, membrane fluidity (Allakhverdiev *et al.*, 2001).

The diel phase following hydration showed expected patterns such as bicarbonate uptake and carbonic anhydrase gene clusters peaking in expression during the photic period (Jensen *et al.*, 2011) (Figure 2b). Similarly, the structural components of the carboxysome also displayed expected expression patterns with expression in the dark as preparation for CO_2 uptake during the next photic period. The transcriptional regulation of photosynthetic activity during the diel cycle may be via the *sufSDCB-sufR* genes (Figure 2b), potentially involved in FeS cluster generation for the photosynthetic apparatus (Wang *et al.*, 2004), and also via expression of the *psII–psaL* gene cluster. The cyclical nature of temperature, light and oxygen concentrations was also reflected in the expression of genes related to heat or oxidative stress response such as the chaperones and ROS scavengers. The dark phase upregulation of a gene cluster homologous to gas vesicle proteins was surprising as *M. vaginatus* is not known to synthesize these buoyancy-providing structures, although some of the genes essential to their formation (*gvpJ-M-O*) were not identified (Offner *et al.*, 2000).

The onset of dehydration triggered the down-regulation of genes involved in several pathways that corresponded to a decrease in metabolism, and also the upregulation of genes that were required to prepare for desiccation (Figure 2c). Although *M. vaginatus* employed several strategies to deal with desiccation, we observed continued CO_2 fixation (and respiration) even as bulk soil water potentials reached -40 to -95 MPa (approximately water content values of 1.5% and 0.5%) (Supplementary Tables S1 and S2, Supplementary Figure S1). Previous work (Brock, 1975) has demonstrated that photosynthesis ceases when *M. vaginatus* is exposed to water potentials below -2.8 MPa. Taking into account this observation, and the fact that it was done in an axenic culture of *Microcoleus* without its native microbial community and abiotic environment, we hypothesize two explanations for photosynthesis and respiration at water potentials between -40 and -95 MPa. Although, a desiccation stress response was clear from the *M. vaginatus* transcriptome, this cyanobacteria or other organisms from the BSC cryptobiota may have unknown mechanisms that keep water potential higher in the immediate vicinity of the cells allowing the BSC microbial community to support photosynthesis.

Oxidative stress is known to be a primary product of desiccation (Franca *et al.*, 2007) and *M. vaginatus* responded by inducing several genes to scavenge ROS and protect DNA and proteins from oxidative damage and to prevent photo-oxidative damage to reaction centers (Figure 2c). *Microcoleus* PSII reaction centers have been proposed to have a photo-protective mechanism whereby singlet oxygen release is reduced under high-light stress (Ohad *et al.*, 2010). EPS production in UV-B stressed cells of *M. vaginatus* has also been shown to protect against oxidative damage (Chen *et al.*, 2009). Increased expression of chaperones may help reverse any protein unfolding expected to occur during desiccation. Under these conditions proteases may be used to recycle unwanted proteins as part of resource allocation or degrade misfolded proteins. Some genes, such as the *groES/EL* chaperone, orange carotenoid protein and chlorophyll a-/b- binding protein, as well as the regulatory genes *sufR*, GUN4 and TSPO-domain, also showed a diel-expression pattern with increased expression during the day. However, the increase during desiccation was much greater than that seen during diel cycling, likely due to exacerbation of photo-oxidative stress.

Osmotic balance is likely maintained initially through cation transport using Na^+/H^+ exchangers or K^+/H^+ antiporters that can be regulated by ChaB domain transport regulators (Osborne *et al.*, 2004) (Figure 2c). As desiccation stress intensified, genes for the synthesis of compatible solutes, trehalose and sucrose (Hagemann, 2011) were induced. Our results suggest a turnover of glycogen, while reserving nutrients and energy in the form of cyanophycin, poly-hydroxy-alkanoates and polyphosphate, during desiccation (Figure 2c).

Transcriptional events during dehydration also suggest processes that may poise the cells for resuscitation. The expression of transporters for the uptake of sugars during drying may be important in competing for extracellular compatible solutes upon wetting. The upregulation of pentose phosphate pathway, and the polyphosphate glucokinase enzyme (Figure 2c) uniquely induced during drying, provide mechanisms for producing pentose sugars and reducing equivalents (NADPH) both of which are required for the synthesis of nucleotides, and may poise the cell to repair DNA damage during desiccation (Slade and Radman, 2011). Induction of genes in respiration (Figure 2c) may be providing energy required for these anaplerotic reactions. The upregulation of the second carbonic anhydrase specifically during drying may also be for anaplerotic assimilation by phosphoenolpyruvate carboxylase (Giordano *et al.*, 2003; Ye *et al.*, 2008), and it may explain the continued CO_2 uptake seen during drying. The induction of the translation elongation factor EF-G and the GTP binding has been associated with an exit from dormancy (Dworkin and Shah, 2010). Analysis of the dry crust at T0 suggested that several RNA transcripts, such as that of the photosystem genes, were stably maintained through dormancy, and this

preparedness may contribute to the fast resuscitation upon hydration.

Our data have helped to uncover several of the likely adaptations that *M. vaginatus* employs to emerge from and re-enter desiccation-induced dormancy. Among the genes that are shared between early cluster A1 and dry-down clusters C1 and C2, 33% and 43%, respectively, of genes are hypothetical or with unknown or uncharacterized domains. Several of these novel genes are likely to have important roles in desiccation survival. The trends in gene transcription observed in response to hydration and dehydration also hint at preparedness for resuscitation. Our data and model provides a foundation for future studies to further explore the genetic basis for adaptation of *M. vaginatus* and BSC communities to their harsh ecosystems.

Acknowledgements

We thank Joern Larsen and Hsiao-Chien Lim for analytical assistance. This work was funded through the Laboratory Directed Research and Development Program of Lawrence Berkeley National Laboratory supported by the US Department of Energy under contract number DE-AC02-05CH11231.

References

Allakhverdiev SI, Kinoshita M, Inaba M, Suzuki I, Murata N. (2001). Unsaturated fatty acids in membrane lipids protect the photosynthetic machinery against salt-induced damage in Synechococcus. *Plant Physiol* **125**: 1842–1853.

Belnap J, Gillette DA. (1998). Vulnerability of desert biological soil crusts to wind erosion: The influences of crust development, soil texture, and disturbance. *J Arid Environments* **39**: 133–142.

Belnap J, Warren SD. (2002). Patton's tracks in the Mojave desert, USA: an ecological legacy. *Arid Land Res Management* **16**: 245–258.

Belnap J, Phillips SL, Miller ME. (2004). Response of desert biological soil crusts to alterations in precipitation frequency. *Oecologia* **141**: 306–316.

Belnap J, Phillips SL, Herrick JE, Johansen JR. (2007). Wind erodibility of soils at Fort Irwin, California (Mojave Desert), USA, before and after trampling disturbance: Implications for land management. *Earth Surface Processes and Landforms* **32**: 75–84.

Billi D, Potts M. (2002). Life and death of dried prokaryotes. *Res Microbiol* **153**: 7–12.

Billi D. (2009). Subcellular integrities in *Chroococcidiopsis* sp. CCMEE 029 survivors after prolonged desiccation revealed by molecular probes and genome stability assays. *Extremophiles* **13**: 49–57.

Boschi-Muller S, Gand A, Branlant G. (2008). The methionine sulfoxide reductases: catalysis and substrate specificities. *Arch Biochem Biophys* **474**: 266–273.

Brock TD. (1975). Effect of water potential on a *Microcoleus* (Cyanophyceae) from a desert crust. *J Phycol* **11**: 316–320.

Campbell SE. (1979). Soil stabilization by a prokaryotic desert crust: implications for Precambrian land biota. *Origins Life* **9**: 335–348.

Chakrabortee S, Tripathi R, Watson M, Schierle GS, Kurniawan DP, Kaminski CF *et al*. (2012). Intrinsically disordered proteins as molecular shields. *Mol Biosyst* **8**: 210–219.

Chen LZ, Wang GH, Hong S, Liu A, Li C, Liu YD. (2009). UV-B induced oxidative damage and protective role of exopolysaccharides in desert cyanobacterium *Microcoleus vaginatus*. *J Integr Plant Biol* **51**: 194–200.

Dworkin J, Shah IM. (2010). Exit from dormancy in microbial organisms. *Nat Rev Microbiol* **8**: 890–896.

Franca MB, Panek AD, Eleutherio EC. (2007). Oxidative stress and its effects during dehydration. *Comp Biochem Physiol A Mol Integr Physiol* **146**: 621–631.

Fredrickson JK, Li SM, Gaidamakova EK, Matrosova VY, Zhai M, Sulloway HM *et al*. (2008). Protein oxidation: key to bacterial desiccation resistance? *ISME J* **2**: 393–403.

Garcia-Pichel F, Belnap J. (1996). Microenvironments and microscale productivity of cyanobacterial desert crusts. *J Phycol* **32**: 774–782.

Garcia-Pichel F, Lopez-Cortes A, Nubel U. (2001). Phylogenetic and morphological diversity of cyanobacteria in soil desert crusts from the Colorado plateau. *Appl Environ Microbiol* **67**: 1902–1910.

Garcia-Pichel F, Pringault O. (2001). Microbiology: Cyanobacteria track water in desert soils. *Nature* **413**: 380–381.

Garcia-Pichel F, Wojciechowski MF. (2009). The evolution of a capacity to build supra-cellular ropes enabled filamentous cyanobacteria to colonize highly erodible substrates. *PLoS One* **4**: e7801.

Gibbs AG. (1999). Laboratory Selection for the comparative physiologist. *J Exp Biol* **202**: 2709–2718.

Giordano M, Norici A, Forssen M, Eriksson M, Raven JA. (2003). An anaplerotic role for mitochondrial carbonic anhydrase in *Chlamydomonas reinhardtii*. *Plant Physiol* **132**: 2126–2134.

Golden SS, Canales SR. (2003). Cyanobacterial circadian clocks – timing is everything. *Nat Rev Microbiol* **1**: 191–199.

Granger AC, Gaidamakova EK, Matrosova VY, Daly MJ, Setlow P. (2011). Effects of Mn and Fe levels on *Bacillus subtilis* spore resistance and effects of Mn^{2+}, other divalent cations, orthophosphate, and dipicolinic acid on protein resistance to ionizing radiation. *Appl Environ Microbiol* **77**: 32–40.

Hagemann M. (2011). Molecular biology of cyanobacterial salt acclimation. *FEMS Microbiol Rev* **35**: 87–123.

Hardoim PR, van Overbeek LS, van Elsas JD. (2008). Properties of bacterial endophytes and their proposed role in plant growth. *Trends Microbiol* **16**: 463–471.

Harel Y, Ohad I, Kaplan A. (2004). Activation of photosynthesis and resistance to photoinhibition in cyanobacteria within biological desert crust. *Plant Physiol* **136**: 3070–3079.

Hegde SS, Vetting MW, Mitchenall LA, Maxwell A, Blanchard JS. (2011). Structural and biochemical analysis of the pentapeptide repeat protein EfsQnr, a potent DNA gyrase inhibitor. *Antimicrob Agents Chemother* **55**: 110–117.

Hill DR, Keenan TW, Helm RF, Potts M, Crowe LM, Crowe JH. (1997). Extracellular polysaccharide of *Nostoc commune* (Cyanobacteria) inhibits fusion of

membrane vesicles during desiccation. *J Appl Phycol* **9**: 237–248.
Jensen SI, Steunou AS, Bhaya D, Kuhl M, Grossman AR. (2011). *In situ* dynamics of O_2, pH and cyanobacterial transcripts associated with CCM, photosynthesis and detoxification of ROS. *ISME J* **5**: 317–328.
Kidron GJ, Barinova S, Vonshak A. (2012). The effects of heavy winter rains and rare summer rains on biological soil crusts in the Negev Desert. *Catena* **95**: 6–11.
Kidron GJ, Vonshak A, Abeliovich A. (2008). Recovery rates of microbiotic crusts within a dune ecosystem in the Negev desert. *Geomorphology* **100**: 444–452.
Kidron GJ, Yair A. (2001). Runoff-induced sediment yield over dune slopes in the Negev desert. 1: Quantity and variability. *Earth Surf Process Landf* **26**: 461–474.
Kirilovsky D. (2010). The photoactive orange carotenoid protein and photoprotection in cyanobacteria. *Adv Exp Med Biol* **675**: 139–159.
Klimant I, Meyer V, Kühl M. (1995). Fiber-optic oxygen microsensors, a new tool in aquatic biology. *Limnol Oceanogr* **40**: 1159–1165.
Kohárýová M, Kolárová M. (2008). Oxidative stress and thioredoxin system. *Gen Physiol Biophys* **27**: 71–84.
Kolodny NH, Bauer D, Bryce K, Klucevsek K, Lane A, Medeiros L *et al.* (2006). Effect of nitrogen source on cyanophycin synthesis in *Synechocystis* sp. strain PCC 6308. *J Bacteriol* **188**: 934–940.
Kuroda A, Murphy H, Cashel M, Kornberg A. (1997). Guanosine tetra- and pentaphosphate promote accumulation of inorganic polyphosphate in *Escherichia coli*. *J Biol Chem* **272**: 21240–21243.
Kuske CR, Yeager CM, Johnson S, Ticknor LO, Belnap J. (2012). Response and resilience of soil biocrust bacterial communities to chronic physical disturbance in arid shrublands. *ISME J* **6**: 886–897.
LeBlanc JC, Goncalves ER, Mohn WW. (2008). Global response to desiccation stress in the soil actinomycete *Rhodococcus jostii* RHA1. *Appl Environ Microbiol* **74**: 2627–2636.
Martinez A, Kolter R. (1997). Protection of DNA during oxidative stress by the nonspecific DNA-binding protein Dps. *J Bacteriol* **179**: 5188–5194.
Mayland HF, McIntosh TH. (1966). Availability of biologically fixed atmospheric nitrogen-15 to higher plants. *Nature* **209**: 421–422.
Offner S, Hofacker A, Wanner G, Pfeifer F. (2000). Eight of fourteen *gvp* genes are sufficient for formation of gas vesicles in halophilic archaea. *J Bacteriol* **182**: 4328–4336.
Ohad I, Raanan H, Keren N, Tchernov D, Kaplan A. (2010). Light-induced changes within photosystem II protects *Microcoleus* sp. in biological desert sand crusts against excess light. *PLoS One* **5**: e11000.
Osborne MJ, Siddiqui N, Iannuzzi P, Gehring K. (2004). The solution structure of ChaB, a putative membrane ion antiporter regulator from *Escherichia coli*. *BMC Struct Biol* **4**: 9.
Placella SA, Brodie EL, Firestone MK. (2012). Rainfall-induced carbon dioxide pulses result from sequential resuscitation of phylogenetically clustered microbial groups. *Proc Natl Acad Sci USA* **109**: 10931–10936.
Pointing SB, Belnap J. (2012). Microbial colonization and controls in dryland systems. *Nat Rev Microbiol* **10**: 551–562.
Potts M. (1994). Desiccation tolerance of prokaryotes. *Microbiol Rev* **58**: 755–805.
Pringault O, Garcia-Pichel F. (2004). Hydrotaxis of cyanobacteria in desert crusts. *Microb Ecol* **47**: 366–373.
Richaud C, Zabulon G, Joder A, Thomas JC. (2001). Nitrogen or sulfur starvation differentially affects phycobilisome degradation and expression of the *nblA* gene in *Synechocystis* strain PCC 6803. *J Bacteriol* **183**: 2989–2994.
Scherer S, Ernst A, Chen T, Boger P. (1984). Rewetting of drought-resistant blue-green algae: time course of water uptake and reappearance of respiration, photosynthesis, and nitrogen fixation. *Oecologia* **62**: 418–423.
Slade D, Radman M. (2011). Oxidative stress resistance in *Deinococcus radiodurans*. *Microbiol Mol Biol Rev* **75**: 133–191.
Starkenburg SR, Reitenga KG, Freitas T, Johnson S, Chain PS, Garcia-Pichel F *et al.* (2011). Genome of the cyanobacterium *Microcoleus vaginatus* FGP-2, a photosynthetic ecosystem engineer of arid land soil biocrusts worldwide. *J Bacteriol* **193**: 4569–4570.
Strauss SL, Day TA, Garcia-Pichel F. (2011). Nitrogen cycling in biological soil crusts across biogeography regions in the Southwestern United States. *Biogeochemistry* **108**: 171–182.
Tamaru Y, Takani Y, Yoshida T, Sakamoto T. (2005). Crucial role of extracellular polysaccharides in desiccation and freezing tolerance in the terrestrial cyanobacterium *Nostoc commune*. *Appl Environ Microbiol* **71**: 7327–7333.
Wang T, Shen G, Balasubramanian R, McIntosh L, Bryant DA, Golbeck JH. (2004). The *sufR* gene (sll0088 in *Synechocystis* sp. strain PCC 6803) functions as a repressor of the *sufBCDS* operon in iron-sulfur cluster biogenesis in cyanobacteria. *J Bacteriol* **186**: 956–967.
Ye C, Gao K, Giordano M. (2008). The odd behaviour of carbonic anhydrase in the terrestrial cyanobacterium *Nostoc flagelliforme* during hydration-dehydration cycles. *Environ Microbiol* **10**: 1018–1023.

Supplementary Information accompanies this paper on The ISME Journal website (http://www.nature.com/ismej)